Angewandte Chemie
Eine Zeitschrift der Gesellschaft Deutscher Chemiker

Supporting Information

Room-Temperature Linear Light Upconversion in a Mononuclear Erbium Molecular Complex

*Bahman Golesorkhi, Homayoun Nozary, Laure Guénée, Alexandre Fürstenberg, and Claude Piguet**

anie_201810022_sm_miscellaneous_information.pdf

Experimental Section

The preparation of complex $[Er(\mathbf{L4})_3](ClO_4)_3$ and its exhaustive characterization in term of solid-state structure (CCDC-1834827), stability and solution structure and spectroscopic properties (ESI-MS, NMR, electronic absorption an emission) were reported previously.[17] Solid-state luminescence data were collected on samples mounted directly onto copper plates using conductive silver glue. Emission spectra were measured on a Horiba Scientific Fluorolog 3 spectrofluorimeter equipped with a visible photomultiplier tube (PMT) (220-850 nm, R928P or 185-1010 nm, R2658P; Hamamatsu). The infrared luminescence spectra were recorded using a NIR solid-state InGaAs detector cooled to 77 K (800-1600 nm, DSSIGA020L; Horiba Scientific) and a 850 nm longpass filter (Semrock) upon 801 nm laser excitation. The low-temperature emission spectra were recorded using an optical closed-cycle cryostat capable of reaching low temperatures down to 5 K in a helium atmosphere (Sumitono HC-4E/Janis Research CCS-900/204N). The emission spectra were corrected for the instrumental response function. Resonant excitations into the $Er(^4I_{9/2}\leftarrow{}^4I_{15/2})$ and $Er(^4I_{11/2}\leftarrow{}^4I_{15/2})$ transitions in $[Er(\mathbf{L4})_3](ClO_4)_3$ were achieved respectively with diode lasers MLL-H-800-2.5W (801 nm) and MDL-F-980-10W (966 nm) from Changchun New Industries Optoelectronics Technology Co., Ltd (CNI). A 550/88 nm bandpass filter (Semrock) was placed directly after the sample in visible emission measurements to remove the second-order Rayleigh scattering of the laser line. The excitation beam was loosely focused onto the sample with a 30 cm lens to reach an excitation spot size of ≈1.5 mm in diameter (Surface ≈ 0.07 cm^2). The mathematical analyses were performed by using Igor Pro® (WaveMetrics Inc.), Origin 2017 (OriginLab Corporation) and Excel® (Microsoft) software.

Table S1 Radiative lifetimes calculated using $\frac{1}{\tau_{rad}} = 2303 \cdot \frac{8\pi c n^2 \tilde{\nu}_m{}^2 (2J+1)}{N_A (2J'+1)} \int \varepsilon(\tilde{\nu}) d\tilde{\nu}$ for selected Er(III) excited levels in the complex $[Er(\mathbf{L4})_3](ClO_4)_3$ at 298 K ($\int \varepsilon(\tilde{\nu}) d\tilde{\nu}$ is the integrated spectrum of the incriminated absorption transition recorded in solution, J and J' refer to the ground (J = 15/2) and excited states, respectively, n is the refractive index of the medium, N_A is Avogadro's number, c is the speed of light in vacuum and $\tilde{\nu}_m$ is the barycenter of the transition).[18]

Excited level	$\tilde{\nu}_m$ / cm^{-1}	Radiative lifetime	Solid[a]	CH_3CN[b]
$Er(^4I_{13/2})$	6585	$\tau_{Er,rad}^{^4I_{13/2}}$ /ms	6.3	9.1
$Er(^4I_{11/2})$	10157	$\tau_{Er,rad}^{^4I_{11/2}}$ /ms	5.4	7.8
$Er(^4I_{9/2})$	11494	$\tau_{Er,rad}^{^4I_{9/2}}$ /μs	2.1	3.0
$Er(^4F_{9/2})$	15133	$\tau_{Er,rad}^{^4F_{9/2}}$ /μs	866	1245
$Er(^4S_{3/2})$	18379	$\tau_{Er,rad}^{^4S_{3/2}}$ /μs	716	1029
$Er(^2H_{11/2})$	19037	$\tau_{Er,rad}^{^2H_{11/2}}$ /μs	282	406
$Er(^4F_{7/2})$	20150	$\tau_{Er,rad}^{^4F_{7/2}}$ /μs	405	582

[a] For the solid-state samples, $\tau_{Er,rad}$ was calculated assuming that the structures are similar in different media and taking into account a simple n^3 dependence of the refractive index with n_{solid} = 1.517 and n_{CH3CN} = 1.344.[18] [b] c = 3 mM.

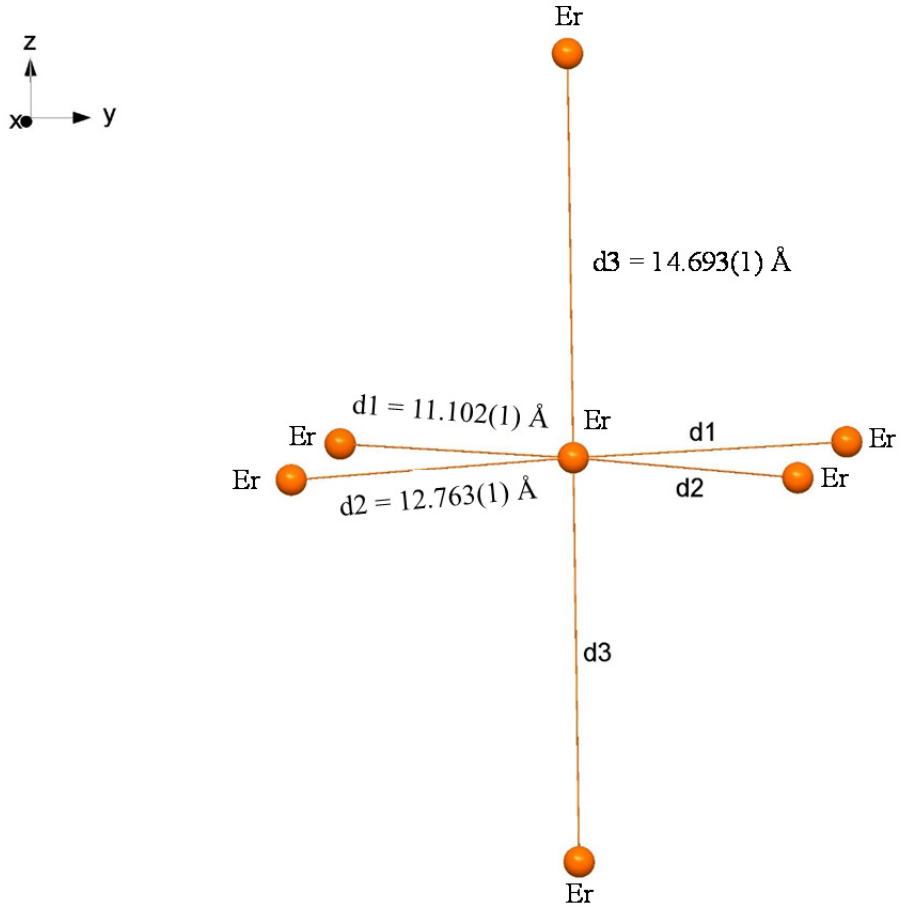

Figure S1. Intermolecular Er···Er distances found in the crystal structures of $[Er(\mathbf{L4})_3](ClO_4)_3 \cdot 1.5CH_3CN$.[17]

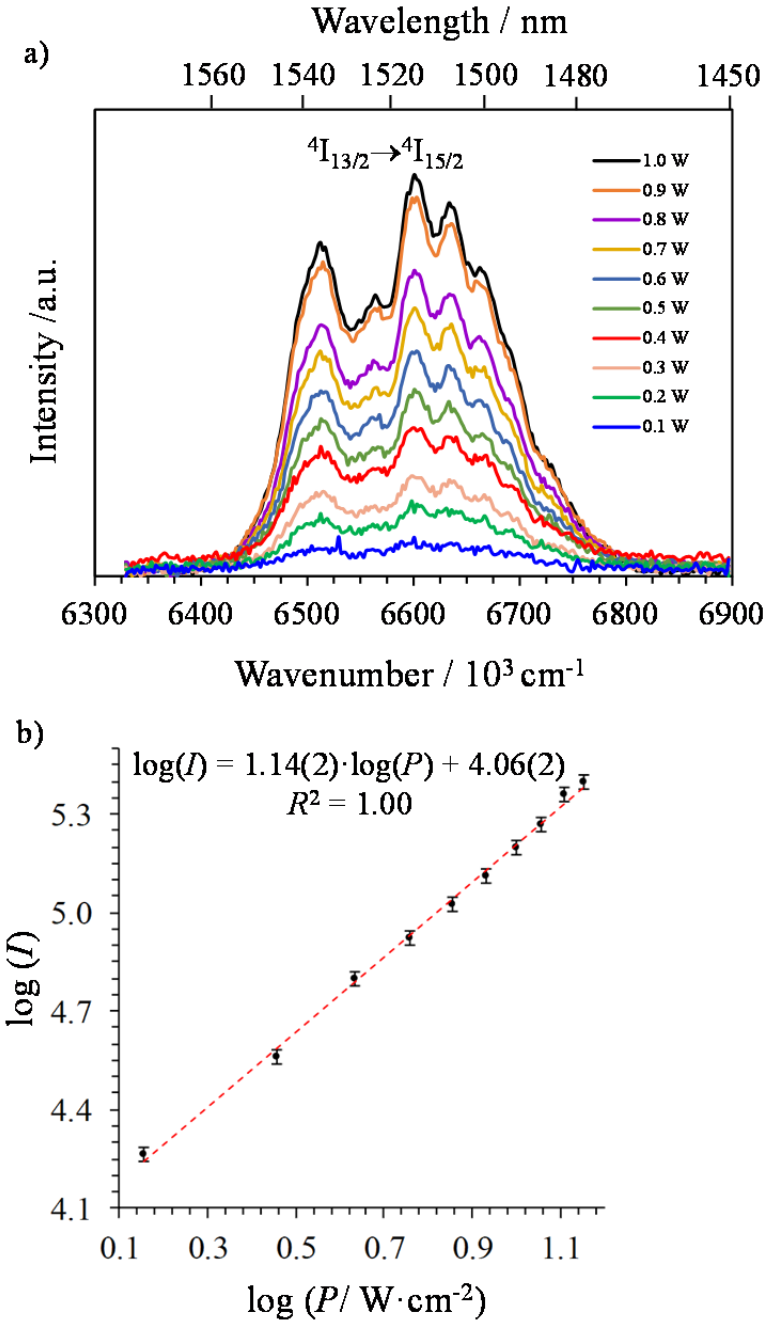

Figure S2. a) Near-infrared downshifted Er($^4I_{13/2}\rightarrow{}^4I_{15/2}$) emission observed for [Er(**L4**)$_3$](ClO$_4$)$_3$ (solid state, 298 K) upon laser excitation of the Er($^4I_{9/2}\leftarrow{}^4I_{15/2}$) transition at λ_{exc} = 801 nm ($\tilde{\nu}_{exc}$ = 12284 cm^{-1}) and for different incident pump intensities focused on a spot size of ≈ 0.07 cm^2 and b) corresponding log-log plot of downshifted intensities *I* as a function of incident pump intensities *P* (in W·cm^{-2}).

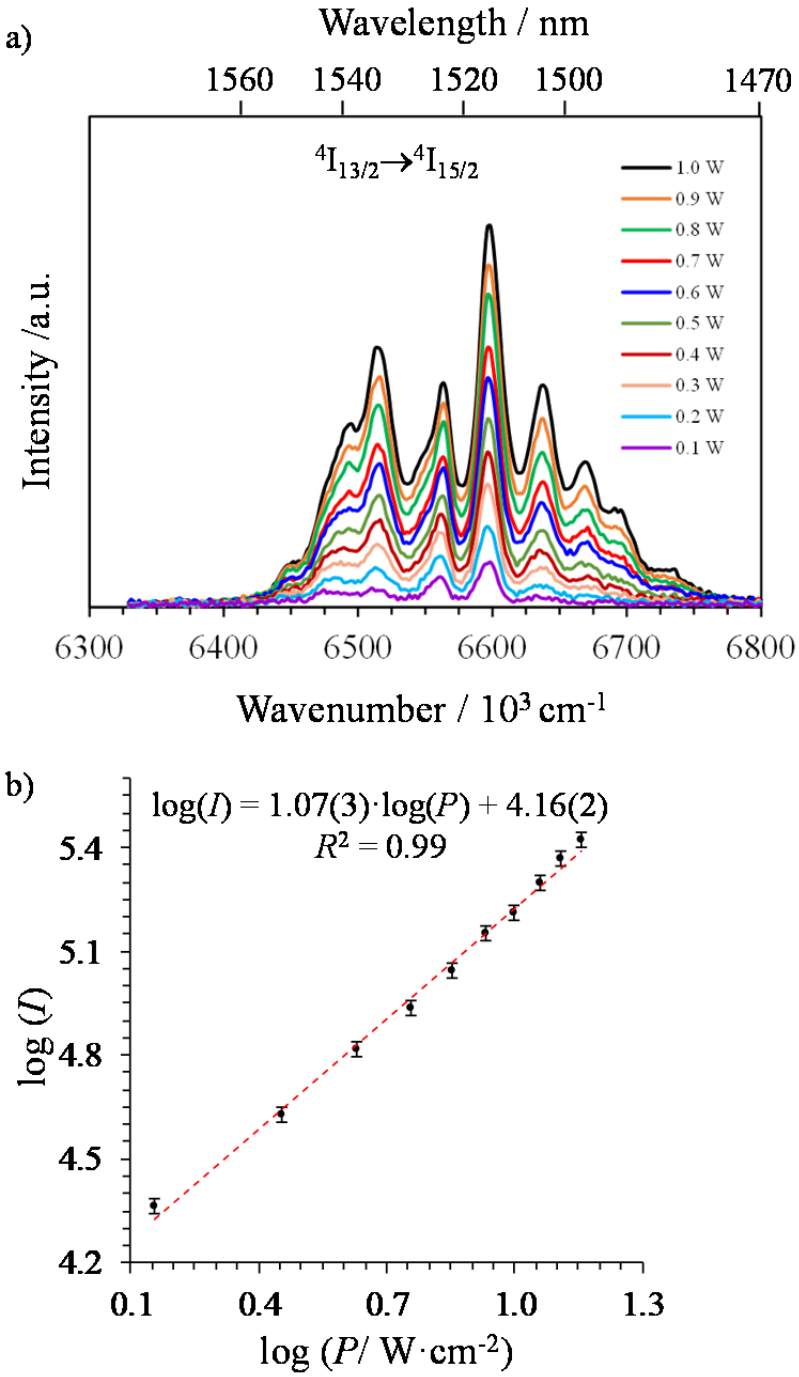

Figure S3. a) Near-infrared downshifted Er($^4I_{13/2}\rightarrow{}^4I_{15/2}$) emission observed for [Er(**L4**)$_3$](ClO$_4$)$_3$ (solid state, 20 K) upon laser excitation of the Er($^4I_{9/2}\leftarrow{}^4I_{15/2}$) transition at λ_{exc} = 801 nm ($\tilde{\nu}_{exc}$ = 12284 cm^{-1}) and for different incident pump intensities focused on a spot size of ≈ 0.07 cm^2 and b) corresponding log-log plot of downshifted intensities *I* as a function of incident pump intensities *P* (in W·cm^{-2}).

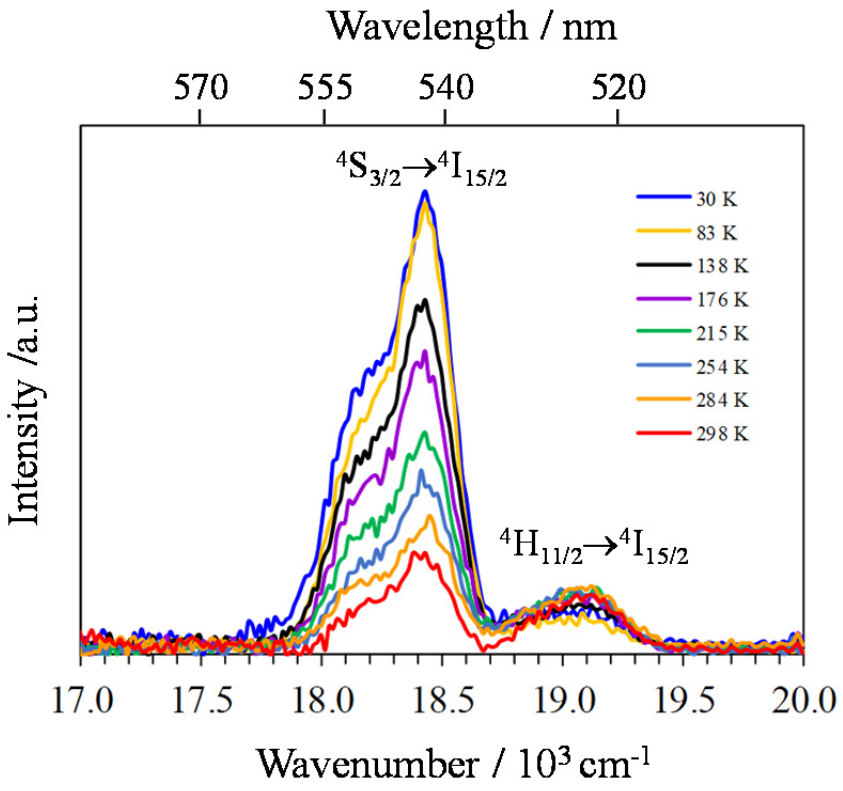

Figure S4. Upconverted visible Er($^2H_{11/2}\rightarrow{}^4I_{15/2}$) and Er($^4S_{3/2}\rightarrow{}^4I_{15/2}$) emissions observed for [Er(**L4**)$_3$](ClO$_4$)$_3$ (solid state, P = 29 W·cm^{-2} focused on a spot size of ≈ 0.07 cm^2) upon laser excitation of the Er($^4I_{9/2}\leftarrow{}^4I_{15/2}$) transition at λ_{exc} = 801 nm ($\tilde{\nu}_{exc}$ = 12284 cm^{-1}) and for different temperatures.

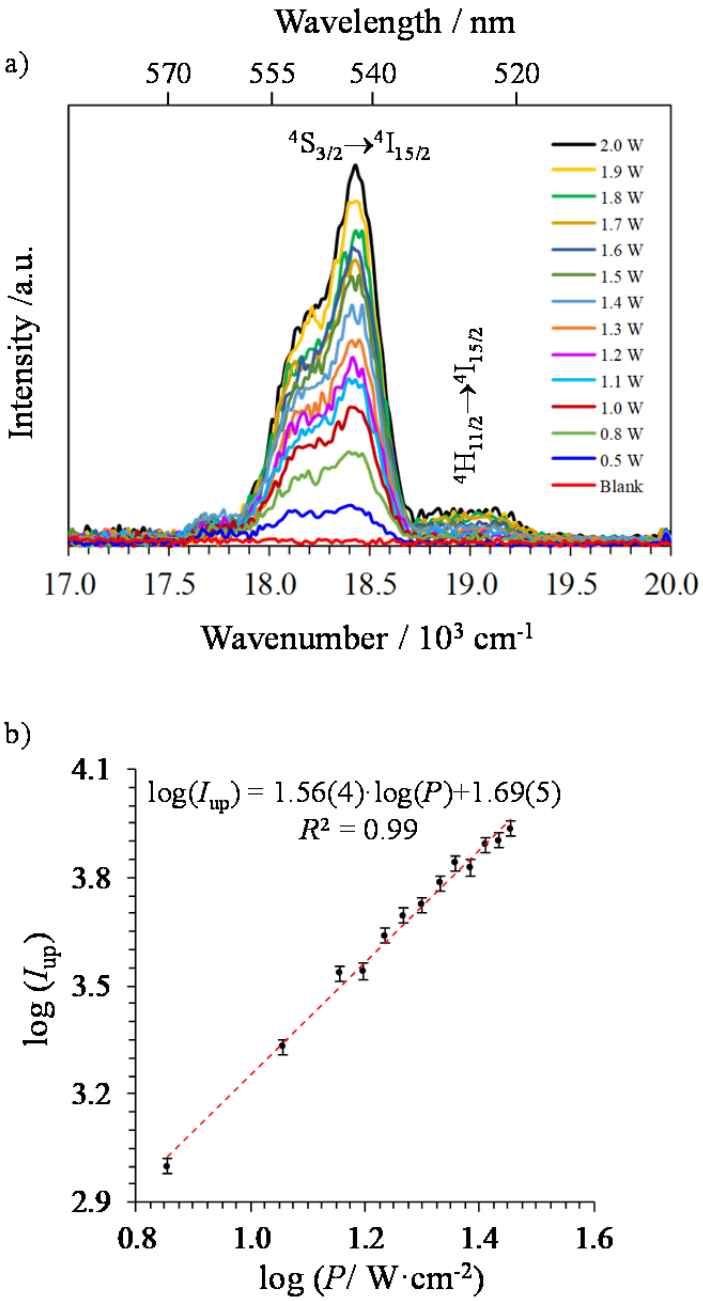

Figure S5. a) Upconverted visible Er($^2H_{11/2}\rightarrow{}^4I_{15/2}$) and Er($^4S_{3/2}\rightarrow{}^4I_{15/2}$) emissions observed for [Er(**L4**)$_3$](ClO$_4$)$_3$ (solid state, 30 K) recorded upon laser excitation of the Er($^4I_{9/2}\leftarrow{}^4I_{15/2}$) transition at λ_{exc} = 801 nm ($\tilde{\nu}_{exc}$ = 12284 cm^{-1}) and using increasing incident pump intensities focused on a spot size of ≈ 0.07 cm^2 (the blank (red curve) was recorded upon irradiation of the copper plate support covered with silver glue at maximum intensity P = 29 W·cm^{-2}) and b) corresponding log-log plot of upconverted intensities I_{up} as a function of incident pump intensities P (in W·cm^{-2}).

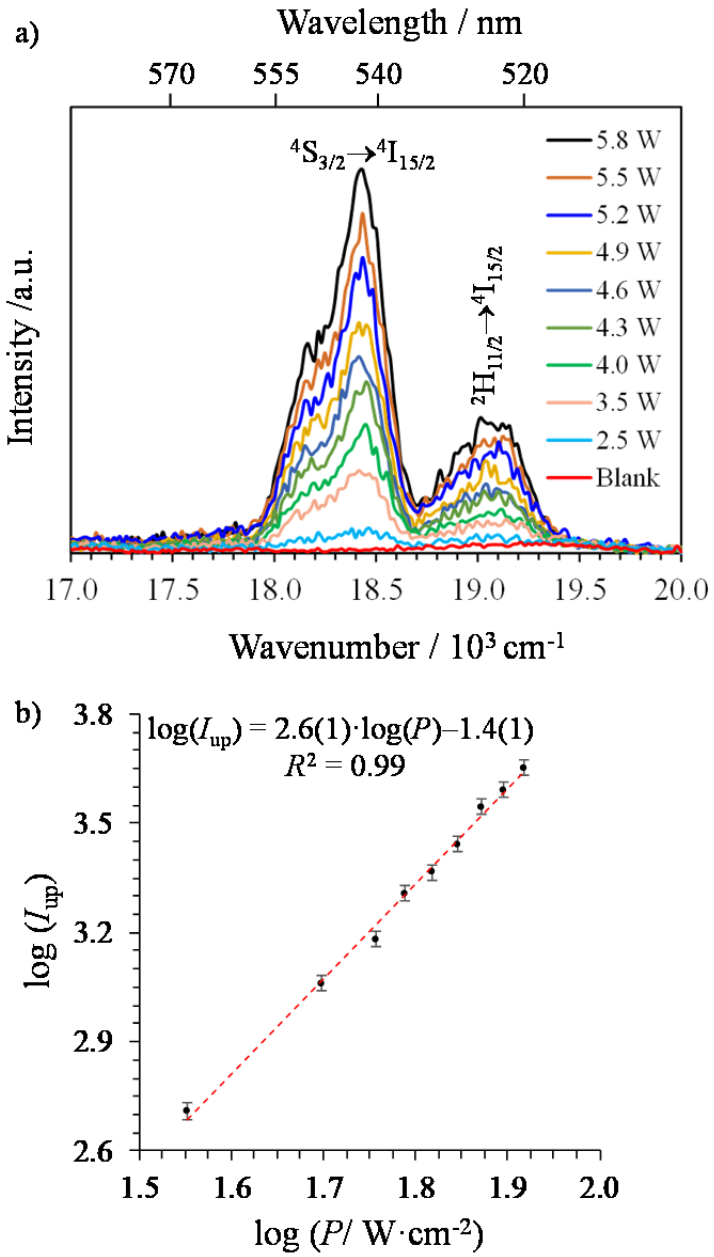

Figure S6. a) Upconverted visible Er($^2H_{11/2}\rightarrow{}^4I_{15/2}$) and Er($^4S_{3/2}\rightarrow{}^4I_{15/2}$) emissions observed for [Er(**L4**)$_3$](ClO$_4$)$_3$ (solid state, 298 K) recorded upon laser excitation of the Er($^4I_{11/2}\leftarrow{}^4I_{15/2}$) transition at λ_{exc} = 966 nm ($\tilde{\nu}_{exc}$ = 10350 cm^{-1}) and using increasing incident pump intensities focused on a spot size of ≈ 0.07 cm^2 (the blank (red curve) was recorded upon irradiation of the copper plate support covered with silver glue at maximum intensity P = 71 W·cm^{-2}) and b) corresponding log-log plot of upconverted intensities I_{up} as a function of incident pump intensities P (in W·cm^{-2}).

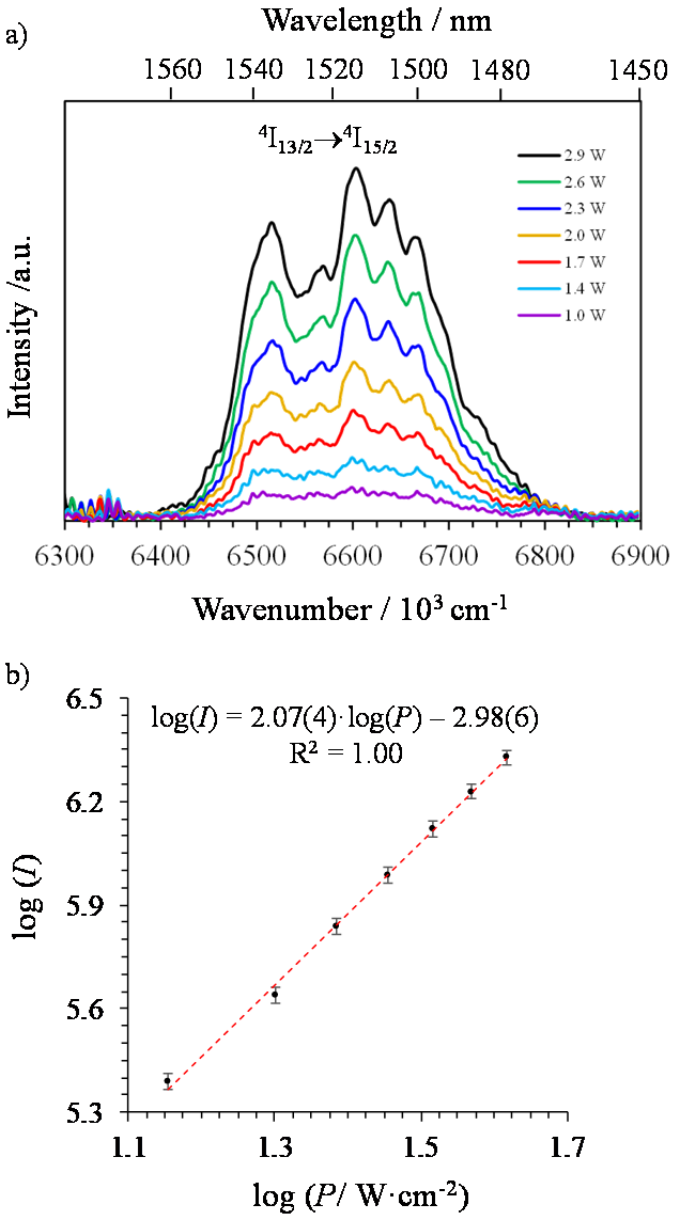

Figure S7. a) Near-infrared downshifted Er($^4I_{13/2}\rightarrow{}^4I_{15/2}$) emission observed for [Er(**L4**)$_3$](ClO$_4$)$_3$ (solid state, 298 K) upon laser excitation of the Er($^4I_{11/2}\leftarrow{}^4I_{15/2}$) transition at λ_{exc} = 966 nm ($\tilde{\nu}_{exc}$ = 10350 cm^{-1}) and for different incident pump intensities focused on a spot size of ≈ 0.07 cm^2 and b) corresponding log-log plot of downshifted intensities I as a function of incident pump intensities P (in W·cm^{-2}).

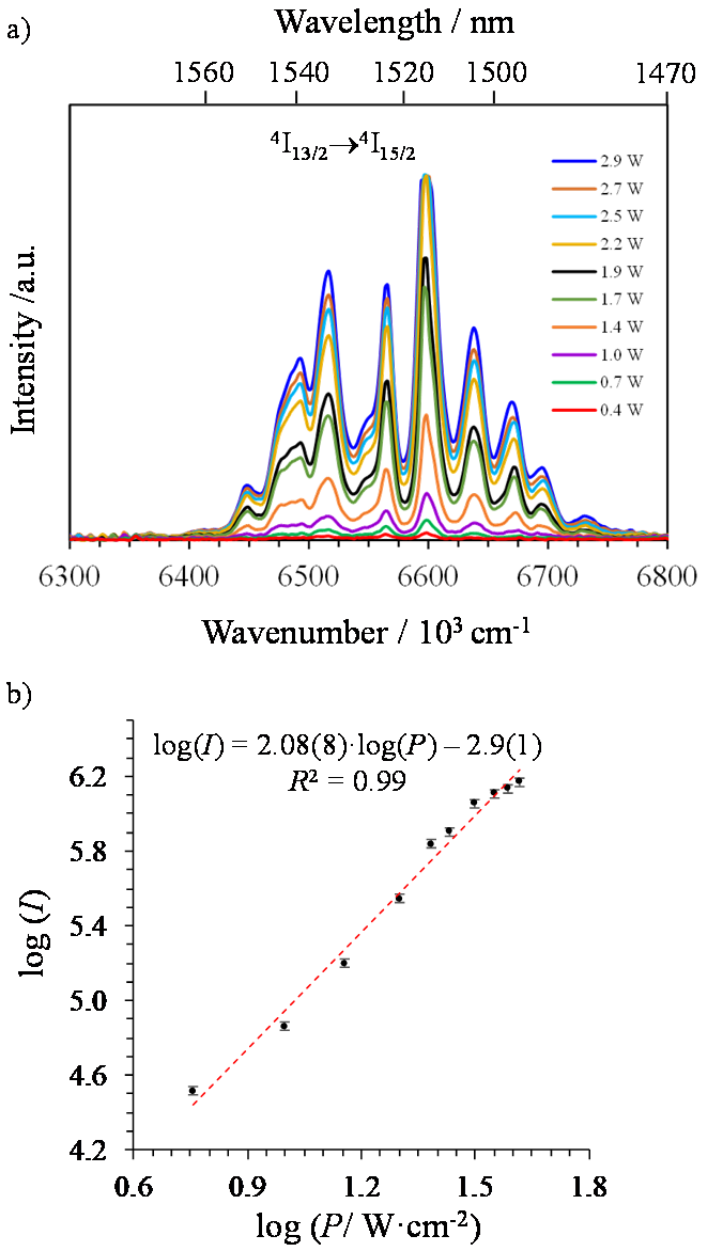

Figure S8. a) Near-infrared downshifted Er($^4I_{13/2}\rightarrow{}^4I_{15/2}$) emission observed for [Er(**L4**)$_3$](ClO$_4$)$_3$ (solid state, 52 K) upon laser excitation of the Er($^4I_{11/2}\leftarrow{}^4I_{15/2}$) transition at λ_{exc} = 966 nm ($\tilde{\nu}_{exc}$ = 10350 cm^{-1}) and for different incident pump intensities focused on a spot size of ≈ 0.07 cm^2 and b) corresponding log-log plot of downshifted intensities I as a function of incident pump intensities P (in W·cm^{-2}).

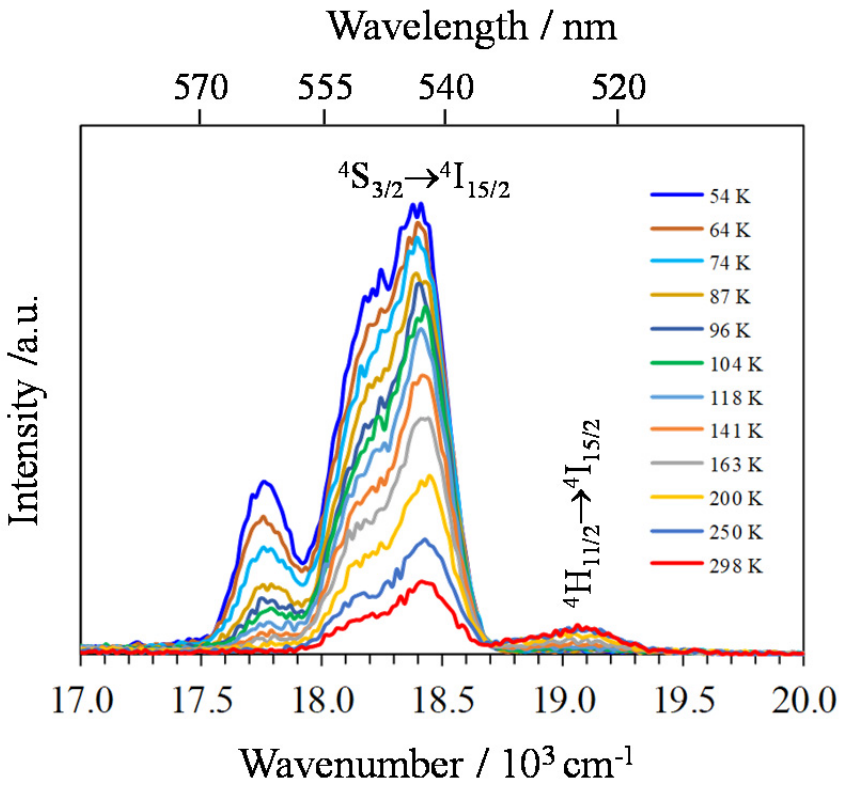

Figure S9. Upconverted visible Er($^2H_{11/2}\rightarrow{}^4I_{15/2}$) and Er($^4S_{3/2}\rightarrow{}^4I_{15/2}$) emissions observed for [Er(**L4**)$_3$](ClO$_4$)$_3$ (solid state, P = 64 W·cm^{-2} focused on a spot size of ≈ 0.07 cm^2) upon laser excitation of the Er($^4I_{11/2}\leftarrow{}^4I_{15/2}$) transition at λ_{exc} = 966 nm ($\tilde{\nu}_{exc}$ = 10350 cm^{-1}) and for different temperatures.

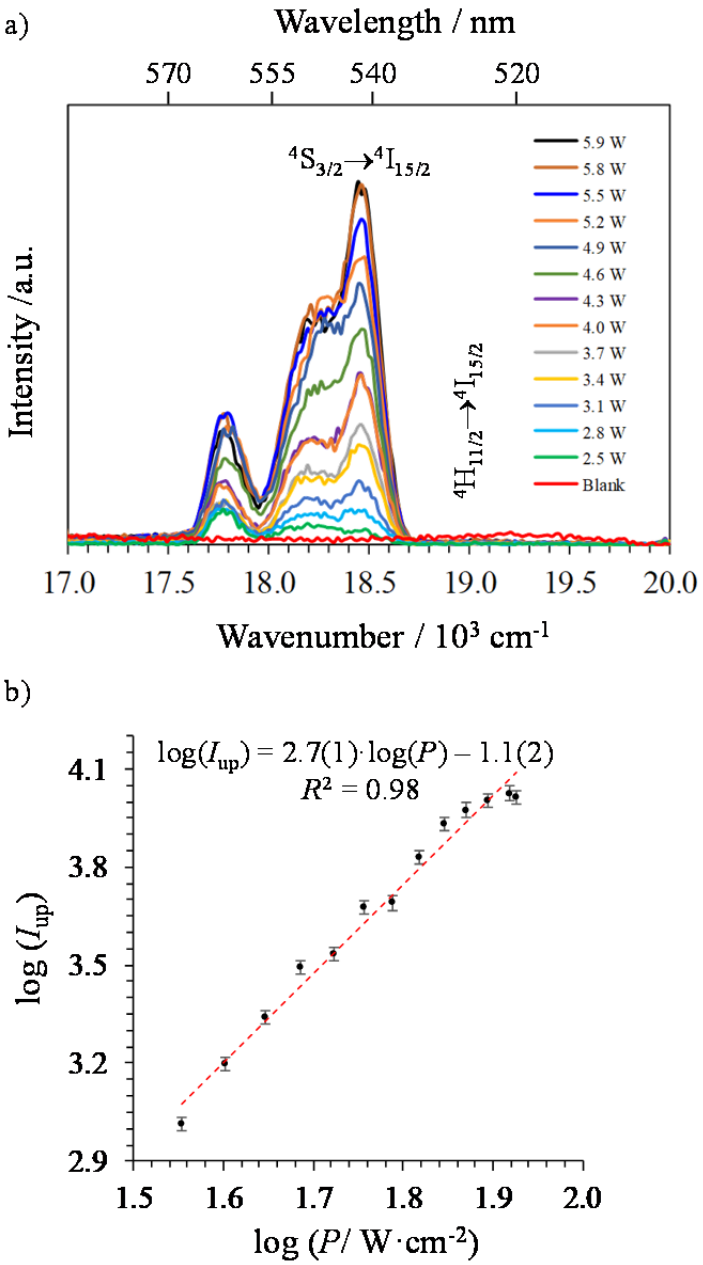

Figure S10. a) Green upconverted Er($^4S_{3/2}\rightarrow{}^4I_{15/2}$) emission observed for [Er(**L4**)$_3$](ClO$_4$)$_3$ (solid state, 52 K) recorded upon laser excitation of the Er($^4I_{11/2}\leftarrow{}^4I_{15/2}$) transition at λ_{exc} = 966 nm ($\tilde{\nu}_{exc}$ = 10350 cm^{-1}) and using increasing incident pump intensities focused on a spot size of ≈ 0.07 cm^2 (the blank (red curve) was recorded upon irradiation of the copper plate support covered with silver glue at maximum intensity P = 71 W·cm^{-2}) and b) corresponding log-log plot of upconverted intensities I_{up} as a function of incident pump intensities P (in W·cm^{-2}).